JNeurosci
THE JOURNAL OF NEUROSCIENCE

Research Articles: Behavioral/Cognitive

Closed-loop slow-wave tACS improves sleep dependent long-term memory generalization by modulating endogenous oscillations

Nicholas Ketz[1], Aaron Jones[2], Natalie Bryant[2], Vincent P. Clark[2] and Praveen K. Pilly[1]

[1]*Information and Systems Sciences Laboratory, Center for Human Machine Collaboration, HRL Laboratories, Malibu, CA 90265, USA*

[2]*Psychology Clinical Neuroscience Center, Department of Psychology, University of New Mexico, Albuquerque, NM 87131, USA*

DOI: 10.1523/JNEUROSCI.0273-18.2018

Received: 30 January 2018

Revised: 31 May 2018

Accepted: 13 June 2018

Published: 23 July 2018

Author contributions: N.A.K., A.J., N.B., V.P.C., and P.K.P. performed research; N.A.K., A.J., N.B., and P.K.P. analyzed data; N.A.K. wrote the first draft of the paper; N.A.K., A.J., N.B., V.P.C., and P.K.P. edited the paper; A.J. and P.K.P. designed research.

Conflict of Interest: All authors listed as affiliated with HRL Laboratories were paid employees during the time of research. PKP has a pending patent application on the closed-loop tACS method.

This material is based upon work supported by the DARPA and the Army Research Office under Contract No. W911NF-16-C-0018. Any opinions, findings, and conclusions or recommendations expressed in this material are those of the author(s) and do not necessarily reflect the views of the DARPA or the Army Research Office.

Corresponding Authors: naketz@hrl.com; pkpilly@hrl.com

Cite as: J. Neurosci ; 10.1523/JNEUROSCI.0273-18.2018

Title Page

Title (50 words max):Closed-loop slow-wave tACS improves sleep dependent long-term memory generalization by modulating endogenous oscillations

Abbreviated title (50 character max): Closed-loop slow-wave tACS improves generalization

Author Names and Affiliations: Nicholas Ketz[1*], Aaron Jones[2], Natalie Bryant[2], Vincent P. Clark[2] and Praveen K. Pilly[1*]

[*]: Corresponding Authors: naketz@hrl.com; pkpilly@hrl.com

[1]: Information and Systems Sciences Laboratory, Center for Human Machine Collaboration, HRL Laboratories, Malibu, CA 90265, USA

[2]: Psychology Clinical Neuroscience Center, Department of Psychology, University of New Mexico, Albuquerque, NM 87131, USA

Number of pages: 34

Number of figures: 6

Number of Words

Abstract: 250

Introduction: 649

Discussion: 1499

Conflict of interest statement:

All authors listed as affiliated with HRL Laboratories were paid employees during the time of research. PKP has a pending patent application on the closed-loop tACS method.

Acknowledgements:

This material is based upon work supported by the DARPA and the Army Research Office under Contract No. W911NF-16-C-0018. Any opinions, findings, and conclusions or recommendations expressed in this

material are those of the author(s) and do not necessarily reflect the views of the DARPA or the Army Research Office.

Abstract

Benefits in long-term memory retention and generalization have been shown to be related to sleep-dependent processes, which correlate with neural oscillations as measured by changes in electric potential. The specificity and causal role of these oscillations, however, are still poorly understood. Here, we investigated the potential for augmenting endogenous Slow-Wave (SW) oscillations in humans with closed-loop transcranial alternating current stimulation (tACS) with an aim towards enhancing the consolidation of recent experiences into long-term memory. Sixteen (three female) participants were trained pre-sleep on a Target Detection task identifying targets hidden in complex visual scenes. During post-training sleep closed-loop SW detection and stimulation was used to deliver tACS matching the phase and frequency of the dominant oscillation in the range of 0.5 to 1.2 Hz. Changes in performance were assessed the following day using test images that were identical to the training ('Repeated'), and images generated from training scenes but with novel viewpoints ('Generalized'). Results showed that active SW tACS during sleep enhanced the post vs. pre-sleep target detection accuracy for the Generalized images compared to sham nights, while no significant change was found for Repeated images. Using a frequency agnostic clustering approach sensitive to stimulation-induced spectral power changes in scalp EEG, this behavioral enhancement significantly correlated with both a post-stimulation increase and subsequent decrease in measured spectral power within the SW band, which in turn showed increased coupling with spindle amplitude. These results suggest that augmenting endogenous SW oscillations can enhance consolidation by specifically improving generalization over recognition or cued recall.

Significance Statement

This human study demonstrates the use of a closed-loop noninvasive brain stimulation method to enhance endogenous neural oscillations during sleep with the effect of improving consolidation of recent experiences into long-term memory. Here we show that transient slow oscillatory transcranial Alternating Current Stimulation (tACS) triggered by endogenous slow oscillations and matching their frequency and phase can increase slow-wave power and coupling with spindles. Further this increase correlates with over night im-

provements in generalization of recent training to facilitate performance in a target detection task. We also provide novel evidence for a tACS induced refractory period following the tACS induced increase. Here slow-wave power is temporarily reduced relative to sham stimulation, which nonetheless maintains a positive relationship with behavioral improvements.

Introduction

Large strides have been made in research surrounding the role of sleep in stabilizing memories. The current model suggests that recent experiences are reactivated during slow-wave sleep, and this reactivation allows for the integration of these experiences into long-term memory. The proposed mechanisms supporting this consolidation suggests that during slow-wave sleep the neocortex begins synchronously oscillating in the Slow-Wave (0.5 to 1 Hz) and Delta bands (1 to 4 Hz). These oscillations are made up of periods of neuronal depolarization accompanied by sustained firing ("Up States") and periods of hyperpolarization associated with neuronal silence ("Down States"). These depolarizing Up States allow for thalamo-cortical spindles (10 to 16 Hz) to emerge in the neocortex, which in turn have been shown to synchronize with hippocampal sharp wave ripples. This has been suggested to facilitate the consolidation of recent experiences, such that ripples indicate hippocampal reactivation, and ripple-spindle-Slow-Wave events mark the transfer of that content to the neocortex (Staresina et al., 2015; Rasch and Born, 2013). The causal role of Slow-Wave (SW) oscillations on spindles and ripples, and the implications of manipulating the endogenous interdependence of each in memory consolidation have yet to be fully explored.

Many studies of sleep-dependent changes in declarative memory show correlations between spindle power and increased "gist" in the learned material rather than recall or recognition. This "gist" has been captured in various ways, including insight into hidden structure of digit strings (Wagner et al., 2004), explicit knowledge of hidden Serial Reaction Time Task response patterns (Fischer et al., 2006), and integration of new words into existing knowledge (Tamminen et al., 2010). These behavioral changes have been shown to correlate with neural oscillations during sleep, suggesting that altering sleep-related neural oscillations could in turn alter the consolidation of these various experiences into existing knowledge.

Indeed, transcranial Alternating Current Stimulation (tACS) has been shown to enhance sleep-dependent

consolidation processes. The dominant paradigms thus far generally use open-loop blocks (5 minutes on, 1 minute off) of 0.75 Hz tACS applied to pre-frontal cortex in non-REM sleep stages N2 and N3. In general, they have shown a selective enhancement for post-sleep declarative memory tasks as opposed to procedural memory tasks (Marshall et al., 2006; Ladenbauer et al., 2017; Westerberg et al., 2015). These results, however, have not been without contention. Some transcranial stimulation studies have yielded null results in both behavior and electrocorticography, casting doubts on the capability for tACS to influence neuronal processing without matching endogenous activity (Lafon et al., 2017; Horvath et al., 2015). These results suggest that stimulation-induced changes in sleep processes can impact behavior, however the specificity of those behavioral changes and the sufficient physiological manipulation are not yet well understood.

Similarly, transcranial Direct Current Stimulation (tDCS) has been shown to influence behavioral performance in a variety of tasks. In particular, Clark et al. (2012) found a stable dose-dependent effect of tDCS on performance such that increasing levels of stimulation improved participants' ability to find hidden targets in complex scenes. This effect was found to persist for at least 24 hours, however no over night changes in performance were found (Clark et al., 2012; Falcone et al., 2012; Coffman et al., 2012). This raises an intriguing question: If tDCS enhanced performance was paired with tACS enhanced sleep-dependent consolidation, could behavioral improvements be further augmented?

This study addresses these open questions by using a novel closed-loop tACS stimulation protocol to target the endogenous SW oscillations during sleep. The influence on behavior is measured in declarative memory through a tDCS enhanced target detection paradigm where participants must learn subtle cues to detect targets hidden in a complex visual environment. Critically, this paradigm has previously shown no over night changes in performance and can assess performance in recognition memory as well as generalization. Here we aimed to show that closed-loop tACS would enhance endogenous SW oscillations driving an improvement in over night memory performance beyond any tDCS related improvements.

Methods

The description of the experimental paradigm and procedures below are also presented in Jones et al. (2018).

Inclusion/Exclusion Criteria

Participants were 18-40 years of age, used English as a first language, completed high school, and had no history of head injury with loss of consciousness for longer than five minutes. They were right-handed according to the Edinburgh Handedness Inventory (Oldfield, 1971), had no history of neurological or psychiatric disorder, had no history of alcohol or drug abuse, were non-smoking, had no excessive alcohol or caffeine consumption, were not currently taking any medication significantly affecting the central nervous system, had no implanted metal, had no sensitivity or allergy to latex, had good or corrected hearing and vision, and reported no sleep disturbances. Women who were pregnant, or thought they may be, were also excluded.

Participants

A total of 21 participants completed the experiment, who were recruited using flyers placed around campus of the University of New Mexico and surrounding community, and received monetary compensation. Four subjects were excluded from the analyses due to equipment failure resulting in relatively fewer stimulation events through their active nights (greater than 1 standard deviation of stimulation counts across the pool), and one subject was excluded due to an unexpected long gap between the acclimation night and the first experimental night. All participants provided signed informed consent to participate in the study, which was approved by the Chesapeake Institutional Review Board. The remaining N=16 participants comprised 3 female, with a mean age of 22.25 years and a SD of 4.96 years.

Target Detection Paradigm

A modified version of the original task, described in Clark et al. (2012), which trained subjects to discover the presence of hidden targets in static images and tracked changes in performance through time, was created to allow for the within-subjects design of the current study. 1,320 still images were extracted from the videos and edited to include or remove specific objects. Targets that were hidden in these images included explosive devices concealed by or disguised as dead animals (e.g., camels), roadside trash, fruit, flora, rocks, sand, or building structures; and enemies in the form of snipers, suicide bombers, tank drivers, or stone-throwers.

The stimulus set was divided into two target categories: people targets (e.g., enemy snipers, friendly fire, etc.), and object targets (e.g., improvised explosive devices, trip wires, etc.). Half of the images presented to participants during testing following training were identical to those seen in training (Repeated images), and half were related, but with varying spatial perspective from the same corresponding scenes (Generalized images). This design allowed for the investigation of effects of the sleep intervention on performance of veridical recall or selective item consolidation in the Repeated images, and of multi-item generalization performance in the Generalized images (Stickgold and Walker, 2013). Participants were instructed that they could stop the task at any time if the stimuli were too uncomfortable, or made them anxious. No subjects elected to stop for such a reason.

Waking Electroencephalographic (EEG) Data Collection

Subjects were prepped and fitted with a neoprene EEG cap that incorporated 32 Ag-AgCl EEG electrodes, placed according to the 10-20 international EEG system (P7, T7, CP5, FC5, F7, F3, C3, P3, FC1, CP1, Pz, PO4, 02, Oz, O1, PO3, CP2, Cz, FC2, Fz, AF3, Fp1, Fp2, AF4, P8, T8, CP6, FC6, F8, F4, C4, P4). Three external channels were utilized, including electrocardiogram (ECG; PO3) placed under the left collarbone, and both vertical (AF3) and horizontal (AF4) electrooculogram (EOG): one placed superior and lateral to the right outer canthus, and another inferior and lateral to the left outer canthus. CMS and DRL reference electrodes were placed on the preauricular. Data were sampled at 500 Hz.

Sleep Polysomnographic (PSG) Data Collection

For polysomnographic (PSG) data collection during sleep, the setup was nearly identical to wake, with a few exceptions. First, two EMG electrodes were placed on and under the chin in accordance with PSG recording guidelines set forth by the American Academy for Sleep Medicine (Berry et al., 2015), to help with sleep scoring. Second, data were collected from 25 EEG electrodes, of which C3, C4, O1, O2 were used for sleep staging. For over night closed-loop SW sleep augmentation, 4 channels dedicated for stimulation were used; namely, F3/F4 place in normal 10-20 positions, and T7/T8 placed on bilateral mastoids. Finally, as F3 and F4 were used for stimulation, they were omitted from data collection; thus, Fp1 and Fp2 were used to assign sleep stages when needed.

Waking Transcranial Direct Current Stimulation (tDCS)

Thirty minutes of continuous transcranial direct current stimulation (tDCS) was delivered via the StarStim R32 simultaneous EEG/Stimulation device (Neuroelectrics, Inc.) during 48 minutes of training. A custom tDCS template for use during awake training was defined in Neuroelectrics control software, CoreGUI. In the active condition a total dose of 1000 μA (1.0 mA) was specified, and for the sham condition a total dose of 100 μA (0.1 mA) was specified. Two electrodes with saline soaked sponges (25 cm^2) were affixed to the participants using a Coban adhesive bandage. In the active condition, the anode electrode was centered over the right sphenoid bone (electrode site F10), and the cathode electrode was placed on the upper contralateral arm. These locations and stimulating amplitudes are based on prior studies using this target detection paradigm (Clark et al., 2012). In the sham condition, the placement, polarities, and duration were identical to the active placement, but the current was set to 0.1 mA instead of 1.0 mA.

Physical sensation ratings were solicited three times during tDCS administration: once after current ramp-up (approximately one minute), four minutes following ramp-up before the first training run began (approximately 5 minutes after stimulation had begun), and immediately following the first training run (approximately 21 minutes after stimulation had begun). Participants were asked to rate three different types of sensations (itching, heat/burning, and tingling) on a 0-10 Likert scale, where 0 indicated no feeling of sensation at all and 10 indicated the worst possible feeling of sensation. Any report of a seven or above resulted in immediate cessation of stimulation and termination of the experiment, without penalty to the participant.

Closed-Loop Transcranial Alternating Current Stimulation During Slow-Wave Sleep

Illustrated in Figure 2, our closed-loop algorithm for electrical augmentation of slow-wave sleep first detects the presence of SW oscillations, which consist of slow synchronized upward and downward deflections of EEG that are associated with memory consolidation. The algorithm next attempts to match the stimulation frequency and phase with ongoing SW activity such that maximal stimulation occurs at the Up States (positive half waves) of the endogenous SW oscillations, as prior work suggests that these are the periods during which coordinated memory replays between hippocampus and neocortex occur to facilitate long-term memory consolidation (Ji and Wilson, 2007). For robust SW detection, a virtual channel is computed

by averaging 13 frontocentral EEG channels (Cz, FC1, FC2, CP1, CP2, Fz, C4, Pz, C3, F3, F4, P3, P4 in the 10-20 system) to determine the overall synchronous activity of EEG recorded during sleep. The virtual channel allows the observation of moments of relatively high SW power, referred to as 'SW events', while averaging out activity of lesser magnitudes on individual channels unrelated to the pattern of SW oscillations. The included channels are stored in a running 5-second buffer. They undergo moving average subtraction with a 1 second window (to mean center the signals at 0 μV), and noisy channels exceeding 500 μV min-to-max amplitude across the 5 seconds are rejected before the virtual channel is computed. The buffer is updated with each discrete data fetch operation that gets the latest data up till the point of that data request. By the time the buffer is updated, there is a random transmission delay, which needs to be accounted for to plan and precisely time the brain stimulation intervention in the near future.

The virtual channel data in the buffer is further processed to actually detect the presence of SW oscillations and possibly predict the upcoming Up State. The algorithm applies a Fast Fourier Transform (FFT) to these stored data to determine the power spectrum. Stimulation is planned when the ratio of the cumulative power in the SW band (0.5-1.2 Hz) is more than 20% of the total cumulative power from 0.1 to 250 Hz. If this SW relative power threshold of 0.2 (or 20%) is crossed, the algorithm then filters the data in the SW band with a second-order, phase corrected Butterworth filter. Next a sine wave is fit to the filtered virtual channel using the identified dominant frequency in the SW band, and with the amplitude, offset, and phase parameter values optimized. The sine wave is then projected into the future, identifying the temporal targets that would synchronize brain stimulation to the predicted endogenous signal. Throughout this process, the dynamic latency associated with data processing is timed using the system clock. Together with distributions of calibrated latencies for data fetch and stimulation commands (mean = 5 ms, SD = 2 ms), which were measured offline, the algorithm determines the correct time point to communicate with the hardware to initiate the stimulation. For instance, suppose at a given moment the algorithm initiates data fetch to populate the buffer with last 5 seconds of EEG data, the data becomes available for processing a few ms (say, 6 ms) into the future based on sampling from the distribution for data fetch latency. Then, say it takes 100 ms for data processing to predict the next Up State, which happens to be 600 ms into the future from the starting time point. If it takes a few ms (say, 7 ms) to physically initiate stimulation based on sampling from the distribution for stimulation command latency, the algorithm would wait 487 ms after the

EEG processing step to send the stimulation command to the device. Ideally, tACS is applied for 5 cycles at the detected SW frequency over bilateral frontal electrodes (F3 and F4) at 1.5 mA per hemisphere with temporal/mastoid returns. Should processing times push beyond any potential stimulation time point, the algorithm compares the current time to the (now deprecated) stimulation time, and checks if at least 300 ms of Up State stimulation is still possible. If so, the stimulation is initiated with an altered start phase (based on the detected SW frequency) for aligning with the endogenous SW Oscillations despite the delay, and is continued until 4 full cycles are completed (where a cycle is defined as the progression from 0° phase to 360° phase). In the event that at least 300 ms of Up State stimulation is not possible, then the algorithm plans the stimulation to start at the next upcoming Up State based on the continued sine wave projections from the buffer. Once stimulation is delivered, the system idles for 3 seconds to avoid the collection of stimulation artifacts in the data buffer, then resumes the cycle of data update in the buffer, data processing and predictions, and stimulation planning as the criteria specified above are met. Our closed-loop system, thus, adapts and adjusts stimulation parameters online in order to ensure the proper administration of stimulation at the correct temporal targets for matching the predicted transient brain states of interest. It is able to minimize the pitfalls of temporal inaccuracies that arise as a result of variable delays intrinsic to any recording/stimulation/processing hardware. On sham nights, Up States were similarly predicted but no stimulation was applied.

Experimental Procedure

The experiment was conducted over the course of six days, including three nights spent in our sleep laboratory referred to here as “acclimation”, “Night 2”, and “Night 3”, two afternoon follow-up testing sessions (“Day 2 Post-Sleep”, “Day 3 Post-Sleep”), as well as an initial orientation session. Participants were randomly assigned to one of four conditions in a within-subjects, counterbalanced, single-blind design: Object Target/Sham Stimulation Night 2, People Target/Active Stimulation Night 3 (SO/AP); Object Target/Active Stimulation Night 2, People Target/Sham Stimulation Night 3 (AO/SP); People Target/Sham Stimulation Night 2, Object Target/Active Stimulation Night 3 (SP/AO); People Target/Active Stimulation Night 2, Object Target/Sham Stimulation Night 3 (AP/SO). At the orientation session, participants were invited to provide informed consent, and were given several questionnaires to assess various aspects of their personal-

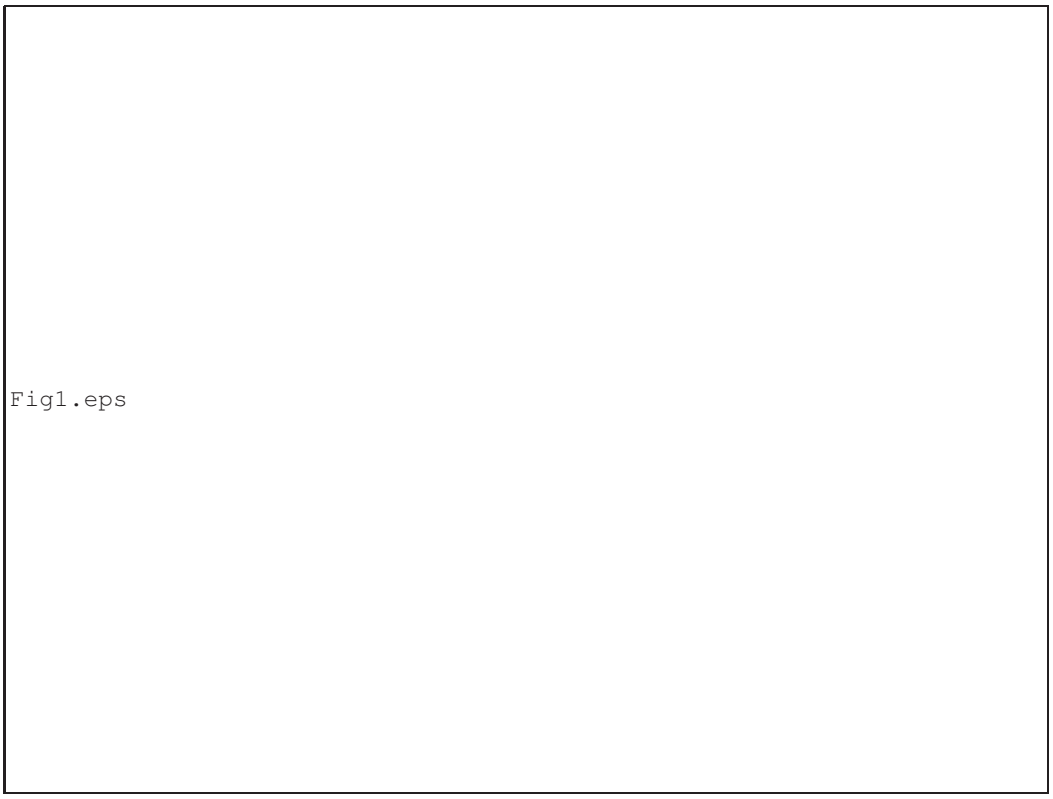

Figure 1: A) Target Detection task. Participants identified cues of potential targets with binary target present/absent decisions. The study was conducted in multiple phases: baseline (i.e., no feedback on response), Training (video feedback identifying correct and incorrect choices), Immediate Test (no feedback, immediately after training), and Post-Sleep Tests (no feedback, approximately 12 and 24 hours after Training). Active and sham stimulation conditions (counter balanced within-subjects) were administered at training (tDCS) and post-training sleep (closed-loop slow-wave tACS) with the stimulation montage shown in C. B) Memory was tested on two image types: Repeated (identical from training to test) and Generalized (same scene from training to test, but novel spatial viewpoint). C) tDCS montage used for Training shown on left, and tACS montage used for Slow-Wave augmentation during sleep shown on right.

ity and sleep habits, as well as to gather an IQ estimate. Following the questionnaires, head measurements were made (circumference, nasion to inion, and pre-auricular to pre-auricular) to fit an EEG cap. Participants were next given a tour of the sleep laboratories and an explanation of the EEG/Stimulation equipment and experimental procedures. Finally, each participant was issued a Fitbit wrist-worn biometric sensor (Dickinson et al., 2016), with instructions on how to correctly operate it to track sleep prior to their lab

visits.

For the acclimation night, participants arrived at the sleep laboratory by 17:00, and were prepped and fitted with an EEG cap (see Waking Electroencephalographic (EEG) Data Collection Section), and an adapted version of Raven's Progressive Matrices called Sandia Matrices, was administered (Matzen et al., 2010). Next, data was collected to calibrate biometrics for use in a predictive computational model, including a breath count task to measure attentional lapses (Braboszcz and Delorme, 2011) that lasted 30 minutes, as well as a 3-back task to generate cognitive stress and mental fatigue (Hopstaken et al., 2015) that lasted 21 minutes was gathered. Participants could then relax in the laboratory until roughly 21:00, when they were prepped for PSG recording during sleep (See Polysomnographic Data Collection Section). EEG electrode locations were digitized using Polhemus FASTRAK System (Polhemus, Inc.) for data analysis purposes as well as to measure how much the cap may have shifted during the subsequent sleep episode. Participants were instructed to lie down in a supine position at approximately 22:00, when biocalibrations were performed to help identify sources of noise in later EEG acquisition. This included EEG data collection of eyes open for 1 minute, closed for 1 minute, looking up, down, right, and left, blinking slowly 5 times, clenching the jaw, and finally moving into a comfortable sleeping position. Lights out for the participants occurred between 22:00-23:00, and they slept for up to 8 uninterrupted hours before being awoken. During sleep, EEG data were monitored, and the closed-loop prediction algorithm was started when 4 minutes of continuous, visible N2/N3 sleep was observed by a trained research assistant. During the acclimation sleep, no stimulation was applied, but the information gathered from the closed-loop prediction algorithm was used to verify the SW relative power threshold of 0.2 for subsequent experimental nights for each participant. Upon waking, participants could use the restroom, and were offered water and snacks. They filled out the Karolinska Sleep Diary (Åkerstedt et al., 1994) to assess subjective sleep quality. Next, they completed a 1-back task for 21 minutes to assess alertness, and then were disconnected from the EEG hardware, and were released.

For Night 2, subjects arrived at the laboratory at approximately 17:30, and were immediately set up for EEG data collection and tDCS stimulation. Participants were seated in front of the computer and instructed on how to respond to the stimuli, but were not given specific information about the nature of the hidden targets or any strategies with which to find them. First, participants performed two baseline runs, consisting of 60 images per run, and made a binary response (target present/target absent), using the keyboard. Each baseline

run lasted approximately 8 minutes, and no feedback was given regarding performance.

Participants then took a brief baseline mood questionnaire to help assess potential effects of tDCS on subjective mood. The mood questionnaire consisted of nine questions on a 0-5 Likert scale. Items included feelings of nervousness or excitement, tiredness, confusion, sadness, degree of frustration, dizziness, nausea, degree of physical pain or discomfort, and ability to pay attention. After all questions were answered, the training portion of the target detection task was administered.

Participants completed three training runs, the first two of which (training blocks one and two) were under 30 minutes of either low-active (1.0 mA) or sham (0.2 mA) tDCS stimulation, followed by one more run (training block three) immediately following the administration of tDCS. The training blocks differed from the testing blocks in that after each choice, the participants were given audiovisual feedback using a short clip regarding the consequence of their decision. If the participant indicated "target present" and was correct, a short video depicting the mission progressing as planned was shown, with a voiceover praising the participant for choosing correctly. If the participant incorrectly indicated that a target was present, a voiceover chastised them for delaying the mission, or insulted them by indicating they were acting cowardly. If the participant correctly indicated that there was no target present, feedback was given that the mission was progressing as planned. If participants incorrectly indicated that no target was present when in fact there was one, a video showing the consequence of missing the target was shown. For example, another member of the participant's platoon was shot by a sniper, or a Humvee was destroyed by an improvised explosive device. Further, a voiceover scolded the participant for missing the target and told them that members of their team had been killed. Each of the three training blocks consisted of 60 trials each and lasted approximately 16 minutes. Each image was presented for 2 seconds with an inter-trial interval that varied from 4 to 8 seconds. The audiovisual feedback did not provide specific details of the shape or location of the target object, but enough information was available from the test image and feedback movie that the participant could infer the type and general position of the target in the image.

Following the three training runs, two more test runs (testing blocks three and four, referred to as Immediate test) were administered to gauge the immediate effect of tDCS on learning before sleep. Half of the stimuli used in the immediate test had been presented during training (Repeated stimuli), while the remain-

ing stimuli were similar in content and had the same types of targets, but had not been presented during training (Generalized stimuli). Thus, memory for trained images and the generalization of the training to novel images could be examined separately. Following the final test block, participants were administered an exit mood questionnaire consisting of the same nine questions in the initial mood assessment, as well as a questionnaire probing the strategy the participants used to complete the task. Next, a new set of Sandia Matrices was administered, as was a Language History Questionnaire (LHQ). Then participants could relax in the laboratory until roughly 21:00, when they were prepped for PSG recording during sleep (see Sleep Polysomnographic Data Collection Section). EEG electrode locations were digitized, and biocalibrations were performed. Lights out for the participants occurred between 22:00-23:00, and they were allowed again to sleep for 8 uninterrupted hours before being awoken. During sleep, EEG data were monitored, and the closed-loop stimulation intervention was started when 4 minutes of continuous visible N2/N3 sleep was observed, and allowed to run through the remainder of the night. Participants either received closed-loop tACS (1.5 mA/hemisphere) or sham tACS (no current) for the entire duration of sleep (see Closed-Loop Transcranial Alternating Current Stimulation During Slow-Wave Sleep Section for description of the intervention), administered at bilateral frontal anodes (F3 and F4 in the 10-20 system) and temporal/mastoid returns. These locations are based off previous slow-wave sleep interventions (Marshall et al., 2006; Ladenbauer et al., 2017; Westerberg et al., 2015). If the participant showed signs of waking, or needed to use the restroom, the stimulation was paused, and resumed after the participant was again in N2/N3 sleep. Upon waking, participants were allowed to use the restroom, and were offered water and snacks. They filled out the Karolinska Sleep Diary (KSD) to assess subjective sleep quality. Next, for the Day 2 Post-Sleep tests, they first completed two more testing blocks of the target detection task (referred to as Morning test) to assess the effect of SW sleep augmentation on consolidation/performance, filled out the strategy questionnaire, and then were disconnected from the EEG hardware, and released. For the second Day 2 Post-Sleep test, participants arrived approximately 24 hours after their initial Day 1 arrival (17:30), were prepped for EEG data collection, and were administered two more testing blocks (referred to as Afternoon test) to assess the effects of SW sleep augmentation on more long-term retention and performance. Note that each block of test runs (three through eight; i.e., immediate, morning, and afternoon tests) presented 60 Repeated and 60 Generalized images, and there was no overlap in stimuli across these runs.

Approximately 5 days after completing the Day 2 Post-Sleep tests, participants came back to the laboratory for their Night 3 and Day 3 follow-up. The timeline and procedures were identical to Night 2 and Day 2 follow-up, the only differences being the target detection condition (object targets/people targets) and stimulation condition (active/sham) were opposite of their Night 2 assignments. Upon completion of the Day 3 Post-Sleep tests, a final exit questionnaire was administered to gather subjective ratings from participants in terms of how they felt the intervention impacted their memory functioning generally, and they were debriefed, during which time they could ask questions about the nature of the experiment. Please see Figure 1 for a graphical description of the experimental procedures.

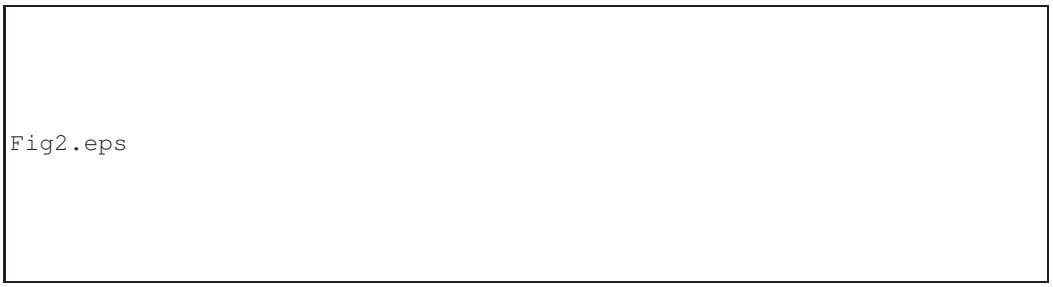

Figure 2: Illustration of the closed-loop system. Left plot shows standard 10-20 electrode montage used during closed-loop tACS, and middle plot shows an example slow-wave detection and prediction from a given subject's sham session (time locked to peak of the targeted Up State). Raw EEG from the teal electrodes shown on the left are minimally preprocessed, then averaged together to form a single Virtual Channel used for Slow-wave detection (shown in light blue). This signal is filtered between 0.5 to 1.2 Hz (shown in dark blue), then used to produce a predictive sine wave fit (shown in green) that is used to schedule the next Up State (shown with the dashed line). The light orange line shows the unfiltered Virtual Channel outside the predictive buffer only available during sham sessions. Right plot shows a group-level Event Related Potential from sham nights centered on the start of the predicted Up States. Red line shows average bandpass filtered voltage in the Slow-Wave band (0.5 to 1.2 Hz) over the within-subject averages shown in grey. Inset plot is the average phase angle at the start of the predicted Up State across subjects. Blue shaded regions show the histogram over 16 subjects, black arrow is average over those subjects, and red shaded region shows 95% confidence around the mean.

Post-Hoc Sleep EEG Analysis

Analysis of the sleep EEG data was performed using custom-built scripts implemented in Matlab R2016a (The MathWorks) taking advantage of various FieldTrip (Oostenveld et al., 2011), and EEGLab (Delorme and Makeig,

2004) functions. EEG data was extracted from sleep sessions and epoched into pre and post stimulation windows, which were in turn triggered by Slow-Wave (SW) oscillations described in the Methods section. The same process was done for the sham condition offline by estimating where stimulation events would have occurred given the on-going SW oscillations, and are synonymously referred to here as 'SW events'. It should be noted these sham SW events were computed post-hoc on the full night's worth of data from the recording session. Indeed the number of SW events significantly varied between active and sham conditions ($t(15) = -8.01,\ p < 0.001$), with 280.87$\pm$45.58 (standard error of the mean) average SW events in the active nights, and 1223.70$\pm$84.32 in the sham nights. An appreciable reason for the discrepancy is that the sham offline code operates on the whole night without any starting latency or pauses, unlike the active online code where the intervention is initiated only after 4 minutes of continuous N2 sleep, and is paused in response to awakenings or any other visual disruption in the participants sleep.

Pre-SW event epochs captured -6.4 s to -0 s before SW event onset, and post-SW event epochs captured 0 s to 12.8 s relative to SW event offset. Here SW event offset occurs after temporal duration of the targeted stimulation for that event, which is 5 cycles at the event specific dominant frequency within the range of 0.5 to 1.2 Hz (i.e., a range from 4.16 to 10 seconds). A segment level artifact removal was done within each epoch by searching in 200 ms sliding windows for a peak to peak voltage change of 500 μV within each channel. Any segment that crossed this threshold was marked as bad and interpolated using non-artifact afflicted time-points before and after the marked segments. Any channel that had more than 25% of its segments within a given epoch marked as bad was discarded and the full epoch for that channel was interpolated using neighboring channels. Any SW event that had more than 80% of its channels exceed the 25% segment threshold were discarded entirely. On average across channels, trials and subjects 15 $\pm$ 22% (here error is 1 standard deviation) of pre-stimulation and 15 $\pm$ 21% of post-stimulation event epoch time points were interpolated in the active condition, and 3 $\pm$ 4% of pre-SW events and 3 $\pm$ 5 post-SW events were interpolated in the sham condition. There were significantly more interpolated events in the active vs. the sham condition (between subjects t-test: pre-SW event $t(15) = 2.56, p = 0.02$, post-SW event $t(15) = 2.48, p = 0.03$). The significantly noisier quality of the active EEG data also contributed to the discrepancy in SW events between active and sham conditions. After segment-level artifact removal, a pass of trial-level removal was done such that any channel that exceeded the 500 μV (min-to-max Voltage

change) threshold within a given SW event was reconstructed by interpolation of its neighbors, and any SW event in which more than 80% of the channels exceeded that threshold the SW event was discarded entirely. Trial sub-selection was done with the constraint that each trial had at least 5.75 s of usable data both pre and post-SW event. On average across subjects, 18 $\pm$ 6% sham and 19 $\pm$ 28% active SW events were discarded due to limited duration, and 10 $\pm$ 8% sham and 18 $\pm$ 20% active SW events were discarded due to more than 80% of channels exceeding artifact threshold. Following artifact removal all epochs were truncated to -6.4 to -1s pre-SW event and 3 to 12.8s post-SW event to ensure no stimulation artifacts lingered in the data. Finally, all epochs were mean centered, bandpass filtered between 0.1 and 125 Hz, bandstop filtered between 59 and 61 Hz, and all channels were re-referenced to the global average across channels.

Spectral Power Methods

Time frequency decomposition was done in FieldTrip using Morelet wavelets. Before decomposition, symmetric (mirror) padding was used to extend the pre and post-SW event time-series to avoid edge artifacts in frequency decomposition. The series of wavelets used in the decomposition started with a width of 4 at the center frequency of 0.5 Hz, and subsequent center frequencies were chosen such that each wavelet was one standard deviation in frequency domain from the previous wavelet. Simultaneously, the wavelet width was increased as a function of center frequency to minimize the combined uncertainty in time and frequency domains, with a starting width of 4 and maximum width of 12. This yielded a time frequency representation with 52 approximately log spaced frequency bins from 0.5 to 100 Hz, and equally spaced time bins of 20 ms. Normalized power within each frequency bin was calculated by first z-scoring within each SW event based on a mean and standard deviation in power estimated over the whole time period (-6.4 to 12.8 s). Relative power within each frequency bin was then calculated using a baseline period across SW events by concatenating -3.5 to -3 s from all pre-SW event periods and estimating a mean and standard deviation from this concatenated time series. These values were then used to z-score within frequency bins both the pre and post periods for each SW event, to avoid single trial bias in spectral normalization (Ciuparu and Mureşan, 2016). This z-scored change in power was then averaged across epochs within the active and sham stimulation conditions separately to yield a single channel $\times$ time $\times$ frequency matrix for each condition and subject.

Phase-Amplitude Coupling Methods

Phase-Amplitude Coupling was estimated using an adaptation of the Oscillation Triggered Coupling (OTC) method as described by Dvorak and Fenton (2014). OTC is essentially an event related potential analysis where the events are time locked to the peaks of high-power events within a targeted frequency band. Summing the voltage signal that is time locked to these events results in a waveform where the peak-to-peak amplitude (referred to as Modulatory Strength) can be used as a measure of how consistently the higher-frequency triggering events fall at a particular phase of the modulating lower-frequency signal. This method was chosen as it allows for estimates of coupling within relatively small window sizes (e.g., less than 2 s). This allowed for a more nuanced temporal analysis necessary given the dynamics of the spectral power results.

To estimate the influence of tACS on the relationship between SW phase and the amplitude of spindle oscillations the temporal onset of high-power events within the range of 8 to 16 Hz were determined using the same variable-width wavelet decomposition methods described in the Spectral Power Methods section. Here approximately log-spaced frequencies from 8 to 16 Hz were estimated from 3 to 10 s every 2 ms to provide the most temporal precision possible given the sampling rate. The spectral estimates were then z-scored over time within each channel $\times$ frequency bin, and peaks within these bins that exceeded a z-score of 2 were used as triggering events. To differentiate where the strongest effects occurred in time, a sliding window with a 1 s duration and a separation (i.e., slide) of 0.25 s was used to segregate triggering events to a given temporal extent. In total 21 overlapping windows were used, starting from 3.5 to 4.5 s and ending at 8.5 to 9.5 s relative to SW event offset. Here our hypothesis was that SW stimulation increased spindle coupling, therefore the voltage signal centered on triggering spindle events was filtered using a phase correcting 2nd order Butterworth filter with passband between 0.5 and 1.2 Hz, as this was the range of frequencies used in tACS. Finally, a 1 second window centered on each of the triggering events for a given channel, modulated-frequency, and temporal extent was summed together to determine the underlying modulating signal, which was then characterized by taking the min-to-max amplitude referred to here as the Modulatory Strength. This yielded a channel $\times$ modulated-frequency $\times$ time matrix for each condition and subject. This measure of Modulatory Strength was z-scored based on an estimate of chance coupling

within each channel $\times$ modulated-frequency $\times$ time bin. Here the same number of triggering events for a given Modulatory Strength estimate were randomly sampled in time to produce an estimate of random coupling within that set of data. This process was repeated 200 times for each Modulatory Strength estimate to determine the mean and standard deviation by which it was z-scored.

Additionally the preferred phase for a given channel $\times$ modulated-frequency $\times$ time bin was estimated by collecting the phase angle from the SW filtered voltage signal centered on each triggering event. The average over this distribution was considered the preferred phase for each bin in the Modulatory Strength matrix of each subject and condition.

Experimental design and statistical analyses

Behavioral performance

To assess waking tDCS related changes in performance a 2 (Stimulation: active, sham) by 2 (Image Type: Generalized, Repeated) ANOVA with a Dependent Variable of F1 score in the Target Detection task was tested as a linear mixed effects model using the lme4 package for R (Bates et al., 2014; R-Core-Team, 2015) and p values for each predictor were estimated using the lmerTest package (Kuznetsova et al., 2015). Similarly, to investigate over night changes in performance a 3 (Test Session: Immediate, Morning, Afternoon) by 2 (Stimulation: active, sham) by 2 (Image Type: Generalized, Repeated) ANOVA with a Dependent Variable of F1 score in the Target Detection task was tested as a linear mixed effects model using the lme4 package for R. This model allowed us to account for the random effects related to individual subjects while also allowing us to include the 4 subjects that had missing data for a single Post-Sleep Test session (2 missing active-Afternoon, 1 missing sham-Morning, and 1 missing sham-Afternoon). Test Session contrasts were coded to compare the average F1 score in the Post-Sleep Tests to the Immediate Test (i.e., Immediate $<$ mean(Morning, Afternoon), referred to as 'Post vs. Pre-Sleep'), and a linear increase with time (i.e., Immediate $<$ Morning $<$ Afternoon, referred to as 'Temporal Increase'). For the over night model, subjects were used as a random factor for the main effects of Stimulation and Image Type (excluded effects from the full random model did not significantly contribute, $\chi^2\,(4) = 4.25,\ p = 0.37$ compared with full model), and fixed effects were defined for the full three-way interaction of Test Session by Stimulation by Image Type.

A similar model was also used for the tDCS effects, with subjects as random factors for the main effects of Stimulation and Image Type. Results from these models are reported here as significant where any predictor reached an alpha level of $p < 0.05$.

Targeted Up State Validation

A test for the precision of the Up State detection algorithm was done using a V-test on the distribution of phase angles within each subject, as well as the distribution of average phase for each subject across the group (Berens, 2009). The null hypothesis of this test was the phase within each subject is either uniformly distributed or not reliable different from the targeted phase of 0.

A test for the distribution of algorithmically detected SW events per sleep stage was done using a linear mixed effects model with the percentage of total SW events over the night broken down by sleep stage as the dependent variable, a fixed effect categorical variable identifying individual sleep stages, and stimulation condition grouped by subjects as a random factor. All but one session was included in this analysis; a single subject's active night sleep stage data was missing and could not be accounted for. Here three specific contrasts were tested to determine if detected SW events were biased to stages N2 and N3. The first compared the average in N2 and N3 with the average over all other sleep stages. The second compared counts in N2 to counts in REM, and the third compared N3 to REM.

Spectral Power and Modulation Strength

Significant changes in relative power and correlations with behavior were estimated using FieldTrip's permutation based clustering algorithm (Maris and Oostenveld, 2007). A contrast of the relative change in power (post-SW event normalized by pre-SW event, as described in EEG Methods section), for the active stimulation condition compared to the relative change in power for the sham condition was made for each channel $\times$ time $\times$ frequency bin between 3 and 10s from offset of SW events. These contrasts were evaluated using a paired t-test over subjects, and a cluster-based permutation test was done to determine the significant channel $\times$ time $\times$ frequency bins. Clusters were created by grouping adjacent bins that had an alpha level of $p < 0.05$. Each cluster was then characterized by the sum of its t-values, and a surrogate distribution of clusters, similarly characterized, was created by shuffling the subject labels and repeating the

clustering procedure 500 times. Thus a clusterwise significance value can be attributed to each observed cluster in reference to its position in the permutation based surrogate distribution. Here we report any cluster that reached a clusterwise significance less than 0.05 (i.e., 95% of the surrogate clusters had smaller summed t-values then the observed cluster). Any contrast cluster that reached this clusterwise threshold was then used as a mask to perform a subsequent cluster based permutation test on the correlation between behavior and the significant channel $\times$ time $\times$ frequency bins. This effectively limits the correlation cluster analysis to the channel $\times$ time $\times$ frequency bins that *a priori* show a significant difference between the active and sham stimulation conditions. Behavioral measures correlated with this masked change in relative power were limited to the measures that showed a significant difference between active and sham conditions, which included: F1 score on Generalized images alone and the interaction of Generalized vs. Repeated images. A separate cluster analysis was done for each of these behavioral measures where correlation coefficients for each significant channel $\times$ time $\times$ frequency bin was calculated within each subject, transformed into a t-value, and adjacent bins that had a significance of $p < 0.05$ were clustered together. The same permutation based significance test was done as in the contrast clusters, where a surrogate distribution of clusters was created by shuffling the subject labels and repeating the correlation clustering procedure 500 times. This number of permutations at the alpha level of 0.05 leads to an expected error of ± 0.01 in the clusterwise p values. This hierarchical clustering procedure focuses on extracted biomarkers that account for performance differences between active and sham conditions are induced by closed-loop tACS, as opposed to biomarkers that are agnostic to brain stimulation.

Significant Modulation Strength (of phase-amplitude coupling between slow-waves and spindles) and its relationship to behavior was determined using a masked cluster based permutation test similar to the method used for spectral power. In this analysis the first-level contrast is between active minus sham conditions using data in the z-scored Modulation Strength matrix. Clusters of channel $\times$ modulated-frequency $\times$ time bins that reach a clusterwise $p < 0.05$ are then passed onto to the masked correlation clustering. Here we again restricted behavioral measures to F1 score on Generalized images and the interaction of Generalized vs. Repeated images.

A test of the significance of preferred phase for Oscillation Triggered Coupling waveforms was done on the distribution of phase angles using Rayleigh's test for non-uniformity with no specific hypothesized mean

direction.

Results

Behavioral Results

tDCS Related Changes

As shown in Figure 3A, active tDCS stimulation showed no significant difference in performance compared with the sham condition ($t(32.9) = 0.881$, $p = 0.385$), and there was no difference in performance for the Repeated vs. Generalized images ($t(29.18) = -1.067$, $p = 0.295$). There was a marginally significant interaction between Stimulation and Image Type ($t(29.35) = -1.90$, $p = 0.067$) such that Repeated images show an increase in performance for active vs. sham tDCS (active=0.81$\pm$0.04 standard error of the mean, sham=0.83$\pm$0.04), while the Generalized images show the reverse (active=0.74$\pm$0.03, sham=0.78$\pm$0.03). To address any concerns regarding outlier subjects, an estimate of each subject's influence on the model was done using Cook's distance. A single subject had a Cook's distance that exceeded 2 standard deviations from the mean distance across subjects. This subject was removed from the model however there was no substantive change in the pattern of results. In general these results suggest there was no reliable effect of tDCS on performance, and if anything tDCS improved Repeated image performance more so than Generalized.

Over night Changes in Behavior

A significant main effect for Image Type ($t(44.36) = -2.74, p = 0.008$) was found, implying that Generalized images, averaged across Test Sessions and Stimulation conditions, had lower F1 score compared with Repeated images. Critically, however, the Post vs. Pre-Sleep by Stimulation by Image Type interaction ($t(143.76) = 2.451, p = 0.015$), and Temporal Increase by Stimulation by Image Type interaction $t(143.76) = 2.457, p = 0.015$) were both significant. Again an estimate of outliers was done using Cook's distance. Again the same subject as the tDCS related changes was determined to be an outlier with a Cook's distance more than 2 standard deviations for the group, and again re-running the model without this

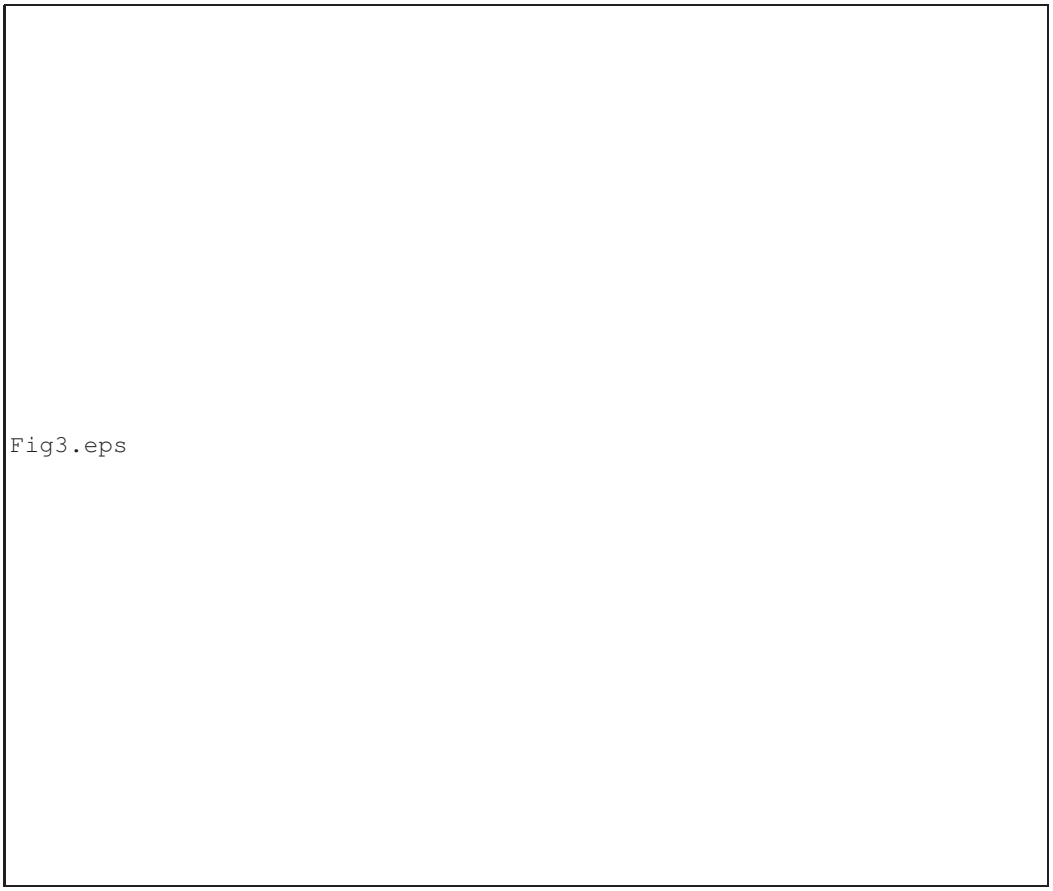

Figure 3: A) Left plot shows the behavioral effects from waking tDCS. Target detection F1 Score from the test immediately following training plotted as an interaction of Image Type by Stimulation condition. No significant main effects were observed, and a marginal interaction was found. Right plot shows over night closed-loop slow-wave tACS effects. Here change in F1 score from average Post-Sleep minus Pre-Sleep performance is shown as an interaction between Image Type and Stimulation condition. Critically, a significant interaction between Image Type and Stimulation condition showed increased over night change in F1 Score for Generalized images in the active condition. Each dot is a given participant's performance, and error bars show standard error of the mean. B) Left plot shows detected Slow-Wave (SW) events broken down per sleep stage as a proportion of the over night total for each subject and condition. Here stages N2 and N3 on average had more SW events than all other stages. Right plot shows total SW events for each stimulation condition. Here active stimulation had fewer total SW events compared to sham. Small dots reflect individual subjects, large dots the group mean, and error bars are boot-strapped 95% confidence intervals.

subject had no substantive change to the pattern of results. This suggests that the change in F1 score after sleep is greater for the active compared to sham Stimulation conditions, and this relationship is contingent upon the test Image Type being Generalized rather than Repeated. A follow up t-test comparing the Post vs. Pre sleep change in F1 score on Generalized images for active vs. sham conditions also showed a significant difference ($t(15) = 2.79, p = 0.014$). These relationships are illustrated in Figure 3B. More detailed behavioral results are presented in Jones et al. (2018).

EEG Results

Slow-Wave Up State Targeted Stimulation

Validation of closed-loop targeted stimulation was done offline using sleep EEG data from sham nights to get an artifact-free estimate of the temporal accuracy of the Up State predictions during the active nights and also to generate SW event markers for sham nights for use in post-hoc EEG analyses. EEG data was extracted in 10 s windows surrounding the start of each predicted Up State as part of the offline code to mark sham SW events. Because of the stochastic delays in the system related to data fetch, processing, and stimulation planning operations, the stimulation doesn't always start at the zero phase of the predicted next Up State. The majority of the stimulation events would be initiated during the first Up State or at the start of the second Up State of the predicted sine wave fit to the endogenous SW oscillations. Therefore, useful averages of consistent phase cannot be made with extracted epochs centered at the start of actual stimulation. To address this, epochs were centered at the start of the first predicted Up State, filtered in the SW band from 0.5 to 1.2 Hz using a phase corrected 2nd order butter-worth filter, Hilbert transformed and again phase corrected by 90 degrees to align with the sine wave prediction used in the closed-loop system. The average phase at the start of the first predicted Up State across events within each subject was calculated and tested against 0; i.e., the intended phase for the start of the positive half waves of the SW oscillations. Using a V-test for circular uniformity (Berens, 2009), each subject rejected the null hypothesis illustrating that the phase within each subject is both non-uniformly distributed and not different from the targeted phase of 0. These average phase estimates are then aggregated across subjects in the polar histogram shown in Figure 2, and the average Event Related Potential (ERP) across events centered at the targeted Up State onset is plotted for each subject as grey lines, with the average over subject ERPs overlaid in red.

Because the closed-loop intervention was allowed to deliver stimulation whenever a SW oscillation reached a sufficient relative amplitude, we assessed the distribution of stimulation events across sleep stages in a post-hoc analysis as illustrated in Figure 3. Here, collapsed across active and sham conditions, the percent of total SW events for a given night averaged over stages N2 and N3 was larger than the average percent of SW events over all other stages ($t(213) = 14.4, p < 0.001$). Further, the percent count in N2 ($t(213) = 10.82, p < 0.001$) and N3 ($t(213) = 3.58, p < 0.001$) were significantly larger than REM.

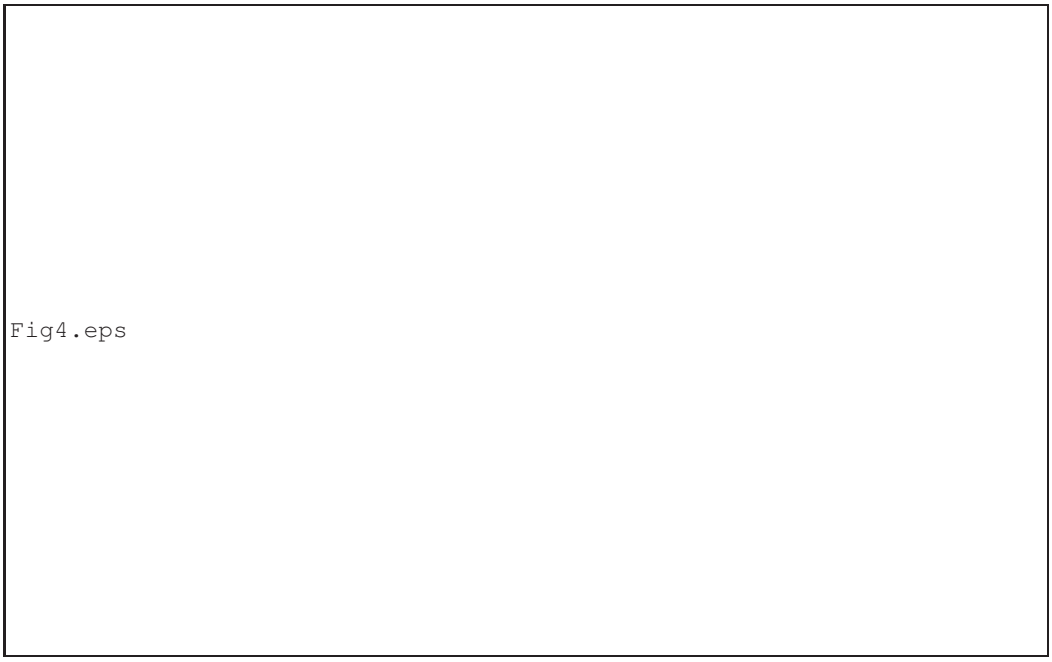

Figure 4: Contrast of relative post slow-wave event power in the active vs. sham conditions. A) Positive cluster showing active greater than sham (clusterwise $p = 0.036$). Upper left plot shows average power difference from significant channel $\times$ time $\times$ frequency bins. Upper right plot shows topography of summed t-values from significant time $\times$ frequency bins. Bottom plot shows t-values from significant time $\times$ frequency bins for each channel. Outlined areas show significant bins and desaturated areas show non-significant bins, with an alpha $p < 0.05$. B) Negative cluster showing sham greater than active with clusterwise $p = 0.008$. Plot layout is the same as in A.

Stimulation-Induced Spectral Power Changes

Post-SW event changes in power were estimated between the active and sham conditions using the clustering procedure described in the Experimental Design and Statistical Analyses section; in short, the contrast of relative post-SW event power in the active vs. sham conditions were clustered between 3 to 10 s post stimulation across all channels and frequencies. Three clusters reached a clusterwise threshold of $p < 0.05$. The first is a positive cluster, i.e., active greater than sham, shown in Figure 4A, with a temporal extent from 3.02 to 4.22 s relative to stimulation offset, a frequency extent from 0.5 to 4.7 Hz, and a clusterwise p value of 0.036. The second is a negative cluster, shown in Figure 4B, with a temporal extent from 4.28 to 9.88 s, a frequency extent from 0.5 to 47.2 Hz, and a clusterwise p value of 0.008. The third is a negative cluster, with a temporal extent from 4.62 to 9.82 s, a frequency extent from 0.5 to 2.6 Hz and a clusterwise p value of 0.047 (this cluster yielded no significant correlations with behavior and is therefore omitted from plots).

Behavioral Correlations with Stimulation-Induced Spectral Power Changes

A similar cluster analysis was done when correlating over night differences (post minus pre-sleep) in F1 score with power changes. However, this analysis was restricted by using the significant contrast clusters as masks to sub-select the channel $\times$ time $\times$ frequency bins used in the correlation with the behavior change differences. Separate correlation cluster analyses were done using each of the significant contrast clusters as a mask and correlating with F1 scores changes from the Generalized images, as well as the interaction between Generalized and Repeated images. In total this yielded 6 follow-up tests.

Correlating the difference in over night F1 score in the Generalized images with each of the significant contrast clusters yielded a significant positive correlation cluster only when using the positive contrast cluster, shown in Figure 4A, as a mask. The correlation cluster, shown in Figure 5A, had a very similar temporal extent to its mask from 3.02 to 4.14s, and a more restricted frequency extent from 0.5 to 2.0 Hz, and a clusterwise p value of 0.002.

Figure 5: Significant ($p < 0.05$) masked correlation cluster results. A) Correlation of spectral power change difference from significant positive contrast cluster bins (Figure 4A) and the over night change (post minus pre-sleep) in F1 score for Generalized images, with a clusterwise $p = 0.002$. Similar to the plot layout in Figure 4, left plot shows average spectral power change difference between active minus sham within the significant correlation cluster bins (desaturated area shows the non-significant bins from the full mask). Illustrative inlay of scatter plot based on average power change difference per subject over all significant bins correlated with over night change in F1 score for Generalized images. Middle plot shows topography of summed t-values from significant time $\times$ frequency bins. Right plot shows time-series of weighted (by summed t-values from significant correlation channel $\times$ frequency $\times$ time bins) average of active and sham power. Significant correlation cluster time points marked in dark shaded region, and error ribbons are standard error of the mean. B) Correlation of spectral power change difference from significant positive contrast cluster bins (Figure 4A) and the over night change difference in F1 score on Generalized images minus Repeated images, with a clusterwise $p = 0.008$. Plot layout the same as in Figure 5A. C) Correlation of spectral power change difference from significant negative contrast cluster bins (Figure 4B) and the over night change difference in F1 score on Generalized images minus Repeated images, with a clusterwise $p = 0.034$. Plot layout is the same as in Figures 5A and B.

Correlating the difference in over night F1 score changes for Generalized images vs Repeated images yielded significant positive correlations when using both the positive (Figure 4A) and negative (Figure 4B) contrast clusters as masks. The positive contrast cluster mask yielded a significant positive correlation, shown in Figure 5B, with a similar temporal extent compared to its contrast cluster mask from 3.02 to 4.06 s, a restricted frequency extent from 0.5 to 0.8 Hz, and a clusterwise p value of 0.008. The negative contrast cluster mask yielded a significant positive correlation, shown in Figure 5C, with a restricted temporal extent compared to its contrast cluster mask from 4.74 to 8.90 s, a restricted frequency extent from 0.5 to 2.0 Hz, and a clusterwise p value of 0.034.

Phase-Amplitude Coupling

Changes in phase-amplitude coupling were assessed using an adaptation of Oscillation Triggered Coupling (OTC) with triggering frequencies from 8 to 16 Hz such that the triggered events were segregated into 1 s windows spaced every 0.25 s, starting from 3.5 to 4.5 s and ending at 8.5 to 9.5 s relative to SW event offset. A comparison between active and sham Modulation Strength was made by calculating the min-to-max amplitude of the OTC waveform filtered in the SW band (0.5 to 1.2 Hz) for each channel $\times$ modulated-frequency $\times$ time bin. Using this data a cluster analysis of Modulation Strength was done in a similar fashion as the spectral power changes.

As shown in Figure 6, the active stimulation condition showed a marginally significant increase in SW phase to high spindle (13 to 16 Hz) amplitude coupling in the time windows centered at 4 and 4.25 s (including all events from 3.5 to 4.75 s), with a clusterwise $p = 0.053$. This increase in active stimulation Modulation Strength highly overlaps in time and spatial topography with the stimulation-induced increase in SW power and its correlation with behavioral changes. The preferred phase of the SW modulating signal in the significant channel $\times$ modulated-frequency $\times$ time bins for the active condition was non-uniformly distributed across events (Rayleigh's test for non-uniformity $r = 7.78, p < 0.001$) and centered at 262°. The preferred phase in the sham condition was not significantly different from a uniform distribution ($r = 0.03, p = 0.85$).

Two other clusters, not shown in the figures, were found with significant decreases in coupling for the active compared to sham conditions. The first spanned from 9 to 16 Hz, and from 6.25 to 7.25 s (including all

events from 5.25 to 8.25 s), with a clusterwise $p = 0.02$. The other spanned 13 to 16 Hz and from 8.5 to 9.0 s (including all events from 8 to 9.5 s), with a clusterwise $p = 0.03$. Both clusters showed a predominant spatial topography over the right central-posterior electrodes, and no significant preferred phase.

A follow-up masked analysis for behavioral correlation was also done using each of the significant clusters found in active vs. sham Modulation Strength, however no significant clusterwise correlation with behavior was found for any of the three masks with F1 score on Generalized images or the interaction between Generalized and Repeated images.

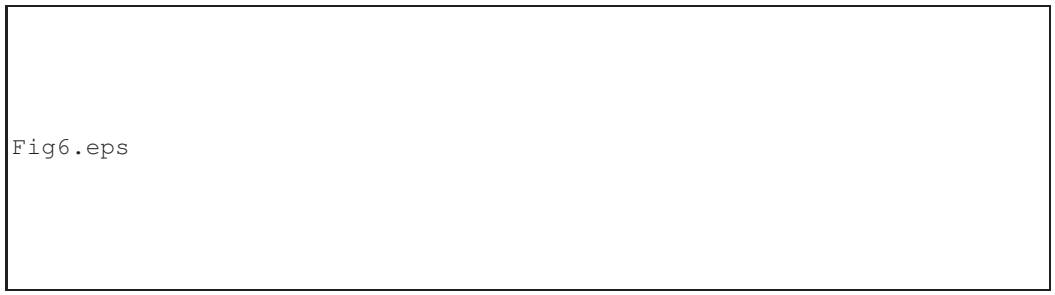

Figure 6: Oscillation Triggered Coupling (OTC) derived measures of phase-amplitude Modulation Strength (min-to-max measures of the average voltage signal temporally centered on high power events within the modulated-frequency, derived from 1 s windows centered on each temporal bin). Here a marginally significant (clusterwise $p = 0.053$) positive cluster shows active stimulation with greater slow-wave Modulation Strength of high spindle (13 to 16 Hz) band amplitude derived from spindle events occurring between 3.5 to 4.75 s relative to slow-wave event offset. Left plot shows summed t-values from significant cluster bins. Middle plot shows individual t-values from the time $\times$ modulated-frequency plots for each channel with the non-significant bins de-saturated. Right plot shows the average slow-wave filtered OTC waveform for active and sham conditions derived from significant cluster bins. These waveforms reflect the summed voltage centered on high power modulating frequency events, which are then averaged over significant cluster bins, and finally over subjects; ribbon is the standard error of the mean over subjects. Inset polar plot shows the average preferred phase for each subject in the active (preferred phase = 262°, $p < 0.001$) and sham (no significant preferred phase) conditions.

Discussion

We have shown that fully closed-loop tACS can be used to effectively target endogenous SW oscillations during natural sleep. This stimulation shows an increase in SW power as late as 4.2 s and is paired with a corresponding increase in coupling with high spindle power. Further, this increase in SW power correlates with behavioral changes in long-term memory performance generally consistent with theories of systems-level consolidation. Moreover we show evidence for a decrease in SW power and coupling with spindle amplitude in active stimulation relative to sham starting around 5 s after stimulation offset. This decrease may be indicative of a SW refractory period induced by stimulation, however these periods still show a positive correlation with behavior such that the longer the stimulation-induced power increase is maintained, the better the post-sleep memory performance.

The use of a frequency agnostic clustering approach in this work adds to the validity of the results, as no *a priori* definition of frequency bands was incorporated into the analysis; however, known biologically relevant frequency bands manifested in the results. Similarly, the focus on stimulation-induced spectral changes through the use of a masked correlation cluster analysis narrows results to those that are related to the stimulation intervention. This not only adds more sensitivity, but allows for more specific interpretation of the changes witnessed. These results help build a better understanding of the potential for improving memory consolidation during sleep and address growing concerns related to the efficacy of tACS to induce physiological and behavioral changes.

Waking tDCS vs. Sleep-dependent Slow-wave tACS

In the present study, no significant effect of tDCS was found with a 1.0 mA current dose, however a non-significant difference in the appropriate direction was observed. It is possible that differences in details of current generation and control between the Iontophoresis systems used previously and the current StarStim system may be involved. Because of this null effect, and previous studies showing no over night change in performance related to tDCS in this target detection task, it is likely that all over night behavioral effects can be attributed to SW tACS.

Given this, it is unclear why there was no improvement in Repeated images induced by SW tACS, as might be expected based on previous studies. Generally, most of these studies have seen effects in some form of a paired-associates task, either word-pairs (Marshall, 2004; Marshall et al., 2006; Westerberg et al., 2015), or visual object paired-associates (Prehn-Kristensen et al., 2014; Ladenbauer et al., 2017, 2016). The target detection task, particularly for the Repeated images, requires participants to find camouflaged targets in complex scenes, and therefore relies more on recognition of perceptual details as compared to standard paired-associates tasks. This may explain why no over night effects were found in the Repeated images alone. In contrast, the strength of the Generalized images in the target detection task is that the performance for a given test cue image is not determined by the best match to the originally studied cue image, but instead its relation to the scene originally studied and the potential for a target to exist in that scene. This provides a much more ecologically plausible memory testing paradigm, allowing for very different perceptual cues to imply the same underlying study item, which is ideal for testing the consolidation of essential 'gist' rather than specific items.

Stimulation-Induced Spectral Power Decreases

The time period and broad frequency range that shows a decrease in SW power for active vs. sham conditions suggests that there may be some stimulation-induced refractory period, and it is unclear how long this period of decreased power lasts. Masked correlation analysis show that this decrease has the same relationship to behavior as the stimulation-induced increases in power shown in Figure 5B and C. This suggests that the stimulation-induced relationship with behavior is relatively constant through-out the analysis window, however the induced power changes start at a level that is higher than the sham nights and slowly decreases over time.

Previous results have shown stimulation induced decreases in SW oscillations. Ngo et al. (2015) applied auditory clicks in predicted Up States to enhance endogenous SW oscillations and found that SW events and spindle-SW coupling decreased as the number of contiguous stimulation events increased. Interestingly they found this decrease did not negatively impact behavior. In reference to our results, this suggests that the stimulation-induced refraction in SW power is a normal self-limiting function, such that large increases in SW power as a result of stimulation are accompanied by periods of suppressed activity.

Previous Sleep-Dependent Memory Enhancing tACS Findings

Several empirical results exist addressing the effectiveness of transcranial Electric Stimulation (tES, here encompassing both direct and alternating current) at inducing measurable electric fields within the brain (Ruhnau et al., 2017; Opitz et al., 2016; Huang et al., 2017; Lafon et al., 2017; Horvath et al., 2015), as well as several studies showing various behavioral changes beyond those targeted here; see Jacobson et al. (2011) for review. The main concerns surrounding the effectiveness of tES is that the induced electric fields are not sufficient to bias network-level firing patterns or oscillations, as is the assumed mechanism of tES protocols. Our approach, however, attempts to target on-going endogenous oscillations, both in frequency and phase, as opposed to inducing them de novo. Based on in vivo studies, the estimated threshold of influence for induced electric fields when attempting to match endogenous activity is 0.25 V/m (Reato et al., 2010; Jefferys et al., 2003; Lafon et al., 2017). Conversely, the measured maximal influence was 0.5 V/m when stimulating at 1.0 mA using a device similar to the Neuroelectrics StarStim device used in this study (Opitz et al., 2016), and 0.4 V/m when stimulating at 2.0 mA using the Neuroconn DC Stimulator Plus (Huang et al., 2017). This suggests our approach has a better chance of inducing measurable oscillatory effects intracranially compared to previous work.

One other study, to our knowledge, has investigated a version of closed-loop tACS with the intent towards enhancing over night memory consolidation. Lustenberger et al. (2016) applied 12 Hz tACS triggered by endogenous spindle (11 to 16 Hz) activity and found a positive influence of stimulation on behavior in a motor memory task but not a declarative memory task. Our study provides a more precise closed-loop system by matching the dominant frequency and on-going phase within the SW band (0.5 to 1.2 Hz), and validates the influence on behavior in a target detection task that is similar to many declarative memory tasks. Moreover, we find effects for a stimulation-induced refractory period that decreases SW power relative to sham but does not disrupt the influence of stimulation on behavior. These results suggest that the longer the stimulation-induced increases in power persist, the better the post-sleep performance on the Generalized images relative to the Repeated images. Further investigations into this phenomenon could provide insight into individual differences in stimulation-induced power changes and its subsequent relationship with behavior.

Spindle Coupling

Here a marginally significant (clusterwise $p = 0.053$) increase in coupling between the phase of the SW band to the amplitude of high spindles for the active condition was found, and this increase was similar to the stimulation-induced window of spatial and temporal increases in SW power that correlated with behavioral improvements. This is consistent with recent results of sleep-dependent consolidation, however the preferred phase in our results is 180° out of phase with the SW Up State (Helfrich et al., 2018; Ladenbauer et al., 2017). Further, a correlation with behavior was not found in these coupling measures, however the overlap in time and spatial topography with the stimulation-induced changes in SW power that did correlate with behavior suggest the increased coupling is potentially related to the behavioral changes. Perhaps the specificity of the high-power spindle events used in the Modulation Strength metric was too broadly defined to reveal correlations with the behavioral measures of interest and center on the SW Up State. Further investigations into these stimulation-induced effects are necessary to integrate with existing results.

Conclusions

In this work and Jones et al. (2018) we focused on building a closed-loop system to better target endogenous oscillations during sleep in hopes of increasing the efficacy of transcranial stimulation on hypothesized systems-level consolidation mechanisms. Through this intervention we showed behavioral changes that were consistent with consolidation theories, and post-stimulation changes in EEG that suggest stimulation-induced enhancement of SW oscillations that positively correlated with those behavioral changes. An increase in SW to spindle coupling was found in an overlapping temporal and spatial topography to the stimulation-induced increases in power and correlation with behavior, suggesting that enhanced SW oscillations lead to an increase in systems-level consolidation processes. We also witnessed apparent stimulation-induced decreases in SW power and coupling with spindles that suggests a reset or refractory period in the endogenous SW oscillations. The positive correlation with behavior persisted into this refractory period, however, and may suggest that individuals less prone to this decrease ultimately show the most improvement in consolidation-related memory performance. The mechanisms that would explain this relationship

with individual differences are unclear, and more investigations into the influence of closed-loop tACS on neuronal processes is required.

References

Åkerstedt T, Hume K, Minors D, Waterhouse J (1994) The subjective meaning of good sleep, an intraindividual approach using the Karolinska Sleep Diary. *Perceptual and Motor Skills* 79:287–296.

Bates D, Mächler M, Bolker B, Walker S (2014) Fitting linear mixed-effects models using lme4. *arXiv preprint :1406.5823*.

Berens P (2009) CircStat: A MATLAB Toolbox for Circular Statistics. *Journal of Statistical Software* 31.

Berry RB, Gamaldo CE, Harding SM, Brooks R, Lloyd RM, Vaughn BV, Marcus CL (2015) AASM scoring manual version 2.2 updates: New chapters for scoring infant sleep staging and home sleep apnea testing.

Braboszcz C, Delorme A (2011) Lost in thoughts: neural markers of low alertness during mind wandering. *Neuroimage* 54:3040–3047.

Ciuparu A, Mureşan R (2016) Sources of bias in single-trial normalization procedures. *Eur J Neurosci* 43:861–9.

Clark VP, Coffman BA, Mayer AR, Weisend MP, Lane TD, Calhoun VD, Raybourn EM, Garcia CM, Wassermann EM (2012) TDCS guided using fMRI significantly accelerates learning to identify concealed objects. *NeuroImage* 59:117–128.

Coffman BA, Trumbo MC, Clark VP (2012) Enhancement of object detection with transcranial direct current stimulation is associated with increased attention. *BMC Neuroscience* 13:108.

Delorme A, Makeig S (2004) EEGLAB: an open source toolbox for analysis of single-trial EEG dynamics including independent component analysis. *J Neurosci Methods* 134:9–21.

Dickinson DL, Cazier J, Cech T (2016) A practical validation study of a commercial accelerometer using good and poor sleepers. *Health Psychology Open* 3:2055102916679012.

Dvorak D, Fenton AA (2014) Toward a proper estimation of phase–amplitude coupling in neural oscillations. *Journal of Neuroscience Methods* 225:42–56.

Falcone B, Coffman BA, Clark VP, Parasuraman R (2012) Transcranial Direct Current Stimulation

Augments Perceptual Sensitivity and 24-Hour Retention in a Complex Threat Detection Task. *PLoS ONE* 7:e34993.

Fischer S, Drosopoulos S, Tsen J, Born J (2006) Implicit Learning–Explicit Knowing: A Role for Sleep in Memory System Interaction. *Journal of Cognitive Neuroscience* 18:311–319.

Helfrich RF, Mander BA, Jagust WJ, Knight RT, Walker MP (2018) Old brains come uncoupled in sleep: slow wave-spindle synchrony, brain atrophy, and forgetting. *Neuron* 97:221–230.

Hopstaken JF, Linden D, Bakker AB, Kompier MA (2015) A multifaceted investigation of the link between mental fatigue and task disengagement. *Psychophysiology* 52:305–315.

Horvath JC, Forte JD, Carter O (2015) Evidence that transcranial direct current stimulation (tDCS) generates little-to-no reliable neurophysiologic effect beyond MEP amplitude modulation in healthy human subjects: A systematic review. *Neuropsychologia* 66:213–236.

Huang Y, Liu A, Lafon B, Friedman D, Dayan M, Wang X, Bikson M, Devinsky O, Parra LC (2017) Measurements and models of electric fields in the in vivo human brain during transcranial electric stimulation. *Brain Stimulation* 10:e25–e26.

Jacobson L, Koslowsky M, Lavidor M (2011) tDCS polarity effects in motor and cognitive domains: a meta-analytical review. *Experimental Brain Research* 216:1–10.

Jefferys J, Deans J, Bikson M, Fox J (2003) Effects of weak electric fields on the activity of neurons and neuronal networks. *Radiation Protection Dosimetry* 106:321–323.

Ji D, Wilson MA (2007) Coordinated memory replay in the visual cortex and hippocampus during sleep. *Nature Neuroscience* 10:100.

Jones AP, Choe J, Bryant NB, Robinson CSH, Skorheim SW, Combs A, Lamphere ML, Robert B, Gill HA, Heinrich MD, Ketz NA, Howard MD, Clark VP, Pilly PK (2018) Effects of Closed-Loop tACS During Slow-Wave Sleep Oscillations Enhances Consolidation of Generalized Information. Manuscript in preparation.

Kuznetsova A, Brockhoff PB, Christensen RHB (2015) Package 'lmerTest'. *R package version* 2.

Ladenbauer J, Ladenbauer J, Külzow N, de Boor R, Avramova E, Grittner U, Flöel A (2016) Transcranial stimulation enhances memory-relevant sleep oscillations and their functional coupling in mild cognitive impairment. *bioRxiv* p. 095588.

Ladenbauer J, Ladenbauer J, Külzow N, de Boor R, Avramova E, Grittner U, Flöel A (2017) Promoting Sleep Oscillations and Their Functional Coupling by Transcranial Stimulation Enhances Memory Consolidation in Mild Cognitive Impairment. *Journal of Neuroscience* 37:7111–7124.

Lafon B, Henin S, Huang Y, Friedman D, Melloni L, Thesen T, Doyle W, Buzsáki G, Devinsky O, Parra LC, Liu AA (2017) Low frequency transcranial electrical stimulation does not entrain sleep rhythms measured by human intracranial recordings. *Nature Communications* 8.

Lustenberger C, Boyle MR, Alagapan S, Mellin JM, Vaughn BV, Fröhlich F (2016) Feedback-Controlled Transcranial Alternating Current Stimulation Reveals a Functional Role of Sleep Spindles in Motor Memory Consolidation. *Current Biology* 26:2127–2136.

Maris E, Oostenveld R (2007) Nonparametric statistical testing of EEG- and MEG-data. *Journal of Neuroscience Methods* 164:177–190.

Marshall L (2004) Transcranial Direct Current Stimulation during Sleep Improves Declarative Memory. *Journal of Neuroscience* 24:9985–9992.

Marshall L, Helgadóttir H, Mölle M, Born J (2006) Boosting slow oscillations during sleep potentiates memory. *Nature* 444:610–613.

Matzen LE, Benz ZO, Dixon KR, Posey J, Kroger JK, Speed AE (2010) Recreating Raven's: Software for systematically generating large numbers of Raven-like matrix problems with normed properties. *Behavior Research Methods* 42:525–541.

Ngo HVV, Miedema A, Faude I, Martinetz T, Mölle M, Born J (2015) Driving sleep slow oscillations by auditory closed-loop stimulation—a self-limiting process. *Journal of Neuroscience* 35:6630–6638.

Oldfield RC (1971) Edinburgh Handedness Inventory.

Oostenveld R, Fries P, Maris E, Schoffelen J (2011) FieldTrip: Open source software for advanced analysis of MEG, EEG, and invasive electrophysiological data. *Comput Intell Neurosci* 2011:156869.

Opitz A, Falchier A, Yan CG, Yeagle EM, Linn GS, Megevand P, Thielscher A, Milham MP, Mehta AD, Schroeder CE et al. (2016) Spatiotemporal structure of intracranial electric fields induced by transcranial electric stimulation in humans and nonhuman primates. *Scientific Reports* 6:31236.

Prehn-Kristensen A, Munz M, Göder R, Wilhelm I, Korr K, Vahl W, Wiesner CD, Baving L (2014) Transcranial Oscillatory Direct Current Stimulation During Sleep Improves Declarative Memory Consolidation in Children With Attention-deficit/hyperactivity Disorder to a Level Comparable to Healthy Controls. *Brain Stimulation* 7:793–799.

R-Core-Team (2015) R: A language and environment for statistical computing [Internet]. Vienna, Austria: R Foundation for Statistical Computing; 2014.

Rasch B, Born J (2013) About Sleep's Role in Memory. *Physiological Reviews* 93:681–766.

Reato D, Rahman A, Bikson M, Parra LC (2010) Low-Intensity Electrical Stimulation Affects Network Dynamics by Modulating Population Rate and Spike Timing. *Journal of Neuroscience* 30:15067–15079.

Ruhnau P, Rufener K, Heinze HJ, Zaehle T (2017) Sailing in a sea of disbelief: In vivo measurements of transcranial electric stimulation in human subcortical structures. *Brain Stimulation*.

Staresina BP, Bergmann TO, Bonnefond M, van der Meij R, Jensen O, Deuker L, Elger CE, Axmacher N, Fell J (2015) Hierarchical nesting of slow oscillations spindles and ripples in the human hippocampus during sleep. *Nature Neuroscience* 18:1679–1686.

Stickgold R, Walker M (2013) Sleep-dependent memory triage: evolving generalization through selective processing. *Nat Neurosci* 16:139–45.

Tamminen J, Payne JD, Stickgold R, Wamsley EJ, Gaskell MG (2010) Sleep Spindle Activity is Associated with the Integration of New Memories and Existing Knowledge. *Journal of Neuroscience* 30:14356–14360.

Wagner U, Gais S, Haider H, Verleger R, Born J (2004) Sleep inspires insight. *Nature* 427:352–355.

Westerberg CE, Florczak SM, Weintraub S, Mesulam MM, Marshall L, Zee PC, Paller KA (2015) Memory improvement via slow-oscillatory stimulation during sleep in older adults. *Neurobiology of Aging* 36:2577–2586.